Two step process for the fabrication of diffraction limited concave microlens arrays

Patrick Ruffieux[1*], Toralf Scharf[1], Irène Philipoussis[1], Hans Peter Herzig[1], Reinhard Voelkel[2], and Kenneth J. Weible[2]

[1]*Institute of Microtechnology, University of Neuchâtel, Rue Breguet 2, CH-2000 Neuchâtel, Switzerland.*
[2]*SUSS MicroOptics S. A., Rue Jaquet-Droz 7, CH-2000 Neuchâtel, Switzerland*
**Corresponding author: Patrick.Ruffieux@unine.ch*

Abstract: A two step process has been developed for the fabrication of diffraction limited concave microlens arrays. The process is based on the photoresist filling of melted holes obtained by a preliminary photolithography step. The quality of these microlenses has been tested in a Mach-Zehnder interferometer. The method allows the fabrication of concave microlens arrays with diffraction limited optical performance. Concave microlenses with diameters ranging between 30 µm to 230 µm and numerical apertures up to 0.25 have been demonstrated. As an example, we present the realization of diffusers obtained with random sizes and locations of concave shapes.

© 2008 Optical Society of America

OCIS codes: (130.0130) Integrated optics, (220.0220) Optical design and fabrication.

References and links

1. D. Daly, R. F. Stevens, M. C. Hutley, and N. Davies, “The manufacture of microlenses by melting photoresist,” Meas. Sci. Technol. **1**, 759-766 (1990).
2. D. Purdy, “Fabrication of complex micro-optic components using photo-sculpturing through halftone transmission masks,” Appl. Opt. **3**, 167-175. (1994).
3. M. T. Gale, G. K. Lang, J. M. Raynor, and H. Schütz, “Fabrication of micro-optical elements by laser beam writing in photoresist,” Proc SPIE **1506**, 65-70 (1991).
4. T.-K. Shih, C.-F. Chen, J.-R Ho, and F.-T. Chuang, "Fabrication of PDMS (polydimethylsiloxane) microlens and diffuser using replica molding," Microelectron. Eng. **83**, 2499-2503 (2006).
5. T.-K. Shih, J.-R. Ho, J.-H. Wang, C.-F. Chen, C.-Y. Liu, C.-C. Chen, and W.-T. Whang, "Fabrication of soft reflective microoptical elements using a replication process," Microelectron. Eng. **85**, 175-180 (2008).
6. D. Chandra, S. Yang, and P.-C. Lin, "Strain responsive concave and convex microlens arrays," Appl. Phys. Lett. **91**, 251912 (2007).
7. X. Dong, C. Du, S. Li, C. Wang, and Y. Fu, “Control approach for form accuracy of microlenses with continuous relief,” Opt. Express **13** 1353-1360 (2005).
8. S.-I. Chang and J.-B. Yoon, “Shape-controlled, high fill-factor microlens arrays fabricated by 3D diffuser lithography and plastic replication method,” Opt. Express **12**, 6366-6371 (2004).
9. T.-H. Lin, H. Yang, and C.-K. Chao, “Concave microlens array mold fabrication in photoresist using UV proximity printing,” Microsyst. Technol. Micro and Nanosystems Information Storage and Processing Systems **13**, 1537-1543 (2007).
10. Y. Xia and G. M. Whitesides, “Soft lithography,” Annu. Rev. Mater. Sci. **28**, 153-84 (1998).
11. Ph. Nussbaum, I. Philipoussis, A. Husser and H. P. Herzig, “Simple technique for replication of micro-optical elements,” Opt. Eng. **37**, 1804-1808 (1998).
12. A. Schilling, R. Merz, Ch. Ossmann, and H. P. Herzig, “Surface profiles of reflow microlenses under the influence of surface tension and gravity,” Opt. Eng **39,** 2171-2176 (2000).
13. D. Malacara and Z. Malacara, *Handbook of lens design*, (Dekker, New-York, 1994).

1. Introduction

For the manufacturing of plano-convex microlens arrays, technologies like, reflow technique [1], grayscale mask photolithography [2] or direct laser writing [3] are well established. The resulting photoresist lens pattern is transferred into the optical substrate like fused silica or silicon, by an additional dry etching step using reactive ion etching (RIE). For the manufacturing of arrays of concave microlenses, the situation is different. While some methods have already been described in literature with different type of material like PDMS

#102197 - $15.00 USD Received 29 Sep 2008; revised 31 Oct 2008; accepted 2 Nov 2008; published 11 Nov 2008

or PMMA [4] [5] [6], only few methods based on the control of the exposure threshold [7] or distribution [8][9] exist to create concave lenses in photoresist. We now propose a novel technology for the manufacturing of high quality concave microlens arrays in this material. This method is based on a two steps photolithography process allowing the formation of highly accurate concave lens shapes ranging from diameters between 30 to 230 µm with diffraction limited properties. Arrays with fill factors up to 80% were realized. Theses lenses can be replicated using soft embossing techniques [10] [11] or could be transferred into fused silica substrates by dry etching. The simplicity of the method was a key point to respect. We tried to avoid additional etching or lift-off steps. Based on this fabrication principle, we also manufactured random diffusers by generating patterns of random locations and sizes of concave resist structures. For laser beam shaping, concave microlenses avoid generating local "hot spots" as convex microlenses do. This is an important advantage for high power laser applications. We first explain the basic principle of the fabrication process and pursue with a detailed explanation of the obtained results. We show that the method allows the fabrication of concave microlens arrays with diffraction limited optical performance. Concave microlenses with diameters ranging between 30 µm to 230 µm and numerical apertures up to 0.25 have been demonstrated. As an example, we present the realization of the diffusers obtained with random sizes and locations of concave shapes.

2. Basic principle

The manufacturing process is based on two steps. Cylindrical holes are produced by photolithography in a photoresist layer. The structures are then melted and hardened by a melting step performed at 150°C for half an hour. The resulting structures have a smooth surface profile as illustrated in Fig. 1.

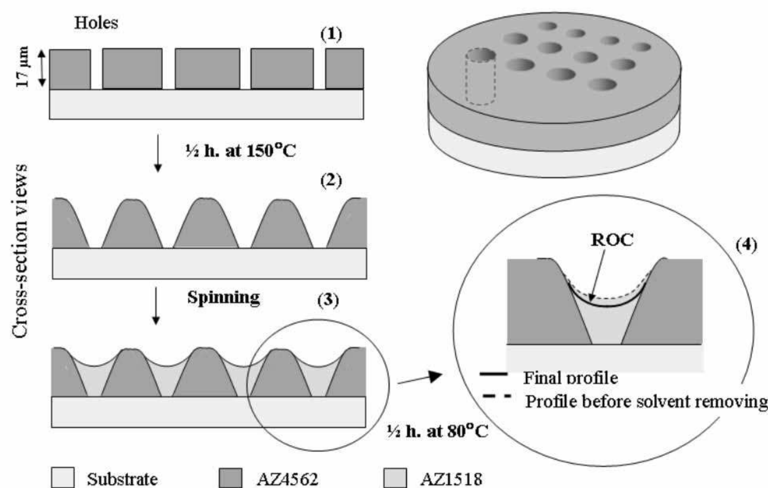

Fig. 1. Process flow. The first step shows a crossed section view of cylindrical holes resulting from a conventional photolithography process (spinning of AZ4562 photoresist, UV exposure through a mask with holes and development). During the second step the holes are melted at 150°C for half an hour. In the third step the holes are filled with AZ1518 photoresist during a second spinning step. To finish, the photoresist is dried in an oven at 80°C for 30 minutes. The concave profile obtained by the surface tension is then modified by the solvent removed in the final cure.

These melted structures are next filled by a second spinning step of resist. After a second bake at 80°C to remove the solvents, concave shapes are generated. Figure 1 shows the process flow. Because of the non-planar surface present during the second spinning step, the spin speed has to be slowed down to allow a homogenous deposition of the photoresist. Thus

#102197 - $15.00 USD Received 29 Sep 2008; revised 31 Oct 2008; accepted 2 Nov 2008; published 11 Nov 2008
(C) 2008 OSA

the final thickness of the photoresist layer is not anymore correlated to the spin speed, but rather to the quantity of photoresist filling the holes.

3. Methodology

A mask containing hole arrays of various diameters has been designed. Hexagonal and square packed holes with diameters in the range between 30 µm to 240 µm spaced by 10 µm were designed. Three additional zones were drawn on the mask with a randomly generated pattern of various hole diameters in the purpose of testing the idea of concave microlens diffusers. As a starting point, the thickness of this first layer on the glass wafer was fixed to 17 µm. To allow spinning of a second layer of photoresist, the first layer of photoresist is baked for half an hour in an oven at 150°C to make it less sensitive to solvent dilution. The melting of the first layer is illustrated in Fig. 2 with pictures of un-melted and melted holes. During melting some reflow of the photoresist structure from thin regions between holes to wider zones occurs [12].

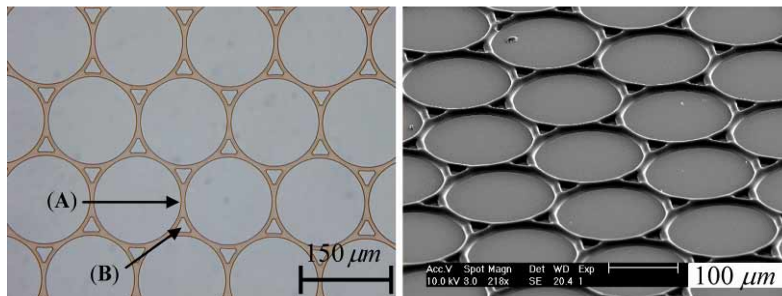

Fig. 2. Microscope picture of unmelted (left) and SEM picture of melted (right) hexagonal packed cylindrical holes of diameter Ø = 150 µm. The height of the walls (A) between holes depends on the reflow process. Empty spaces (B) have been added to the design to reduce reflow and local photoresist peaks formation during the melting step.

The main consequence is, in general, a lower wall ((A) in Fig. 2) between two holes meaning a lower depth of the melted holes. To avoid this drawback a low reflow-sensitive photoresist (AZ4562) has been used. Moreover to reduce this melting drawback, some empty spaces ((B) in Fig. 2) were added to the design of the mask to obtain the same width of the walls everywhere in the photoresist. This effect is shown in detail in Fig. 3. The interference measurements show the phase differences in the hole edges. Because of the too steep slopes of the walls no fringes are resolved. Nevertheless variations on the wall profiles are clearly distinguished. This effect is minimized when employing AZ4562 photoresist instead of AZ9260 photoresist. In the first case only slight deformations of the walls appear visible as dark and light grey modulations. In the second case several black fringes, corresponding to a stronger deformation, are observed. The sag height of these deformations depends on the array geometry. As an example, the height differences between the lowest and the highest part of the wall in Fig. 3 were 3.8 µm in the AZ9260 photoresist and 3 times less around 1.3 µm for the AZ4562 photoresist. The holes are then filled by a second step of spinning. To avoid inhomogeneous deposition of the second layer, some photoresist is poured on all the wafer before spinning occurs. Because of the presence of structures, the spin speed is not anymore correlated to the final layer thickness. In this case it seems correlated to the amount of photoresist left in the filled holes. After filling, the wafers are dried in an oven at 80°C for 30 minutes to remove solvents. At this stage concave shapes are obtained depending on the boundary conditions imposed by the melted holes, the surface tension of the chosen photoresist and the amount of solvent removed during the drying step.

#102197 - $15.00 USD Received 29 Sep 2008; revised 31 Oct 2008; accepted 2 Nov 2008; published 11 Nov 2008
(C) 2008 OSA

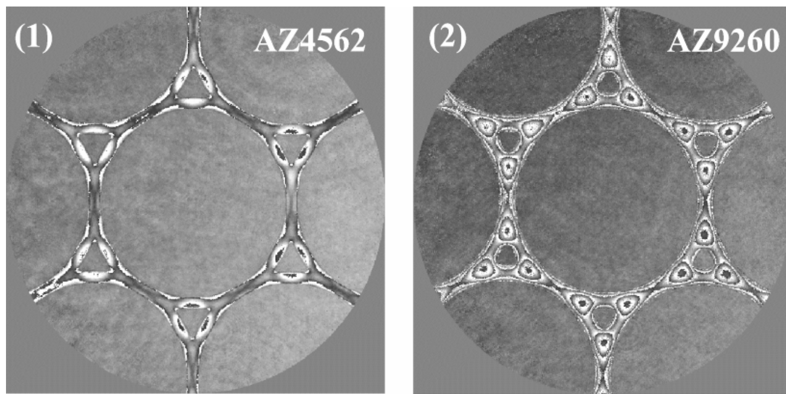

Fig. 3. Illustration of the reflow occurring during the melting step of the first photoresist layer. Using a Mach-Zehnder interferometer two measurements (1) and (2) have been taken. They show interference fringes in the melted walls for two types of photoresist: AZ4562 and AZ9260. While in the first case only one fringe is seen from the lowest to the highest point on the walls more than 3 fringes are distinguished in the second case meaning deformations around 3 times more important.

To evaluate the quality of the resulting concave microlenses, a Mach-Zehnder interferometer was used. According to Marechal's criterion a Strehl ratio > 80 % defines the diffraction limit for lenses [13]. Figure 4 shows in detail the maximum diameter of the diffraction limited concave microlens that have been realized as a function of the spin speed of the second layer of photoresist. Because the master holes are slightly enlarged during the melting step (Fig. 1), the considered concave microlenses have the same diameters that the nominal master hole diameters before the melting step.

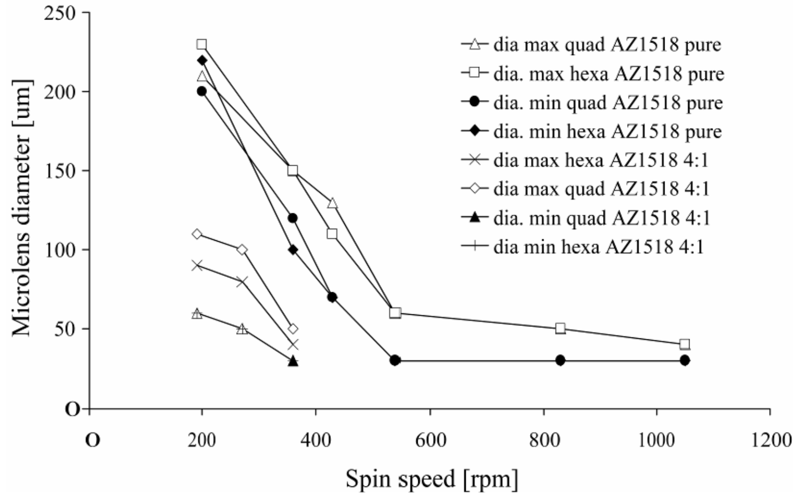

Fig. 4. Results on the fabrication of concave microlens arrays. The curves show the maximum diameters of diffraction limited microlenses that could be obtained when varying the spin speed of the second layer of AZ1518 photoresist. Over this limit, the Strehl ratio of the concave microlenses drops down to values lower than 80%. The minimum diameters were arbitrary set when only one fringe could be solved on the interference measurements or when homogeneity problems happened. Square (quad) and hexagonal (hexa) packed arrays have been considered.

#102197 - $15.00 USD Received 29 Sep 2008; revised 31 Oct 2008; accepted 2 Nov 2008; published 11 Nov 2008
(C) 2008 OSA

It is observed that diffraction limited concave microlens arrays could be produced for diameters in a range between 30 to 230 microns. The minimum achievable diameter was arbitrary defined when only one fringe could be solved (microlens depth > 1.264 µm). Down to this limit, homogeneity problems related to the resist filling of the holes occur. For diameters over 150 µm, diffraction limited microlenses are only achievable when the holes are almost filled, resulting in a nearly flat profile. The numerical aperture (NA) is then lower than 0.02. The numerical aperture can be modified by changing the spin speed and/or the dilution of the photoresist as seen in Fig. 5 and Fig. 6.

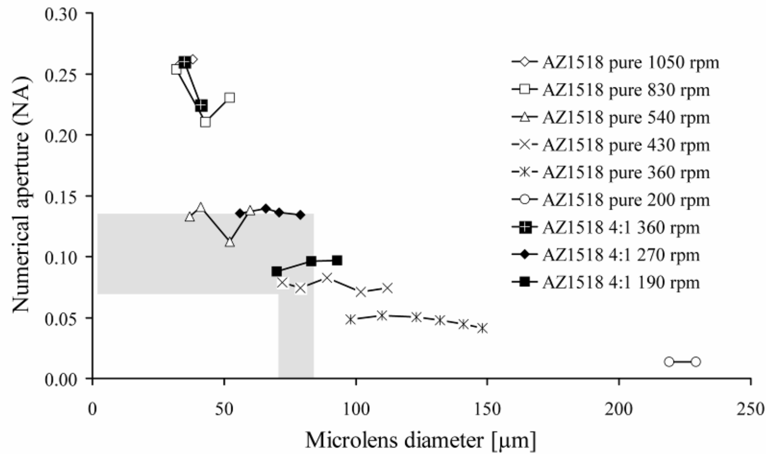

Fig. 5. Numerical aperture (NA) as function of the microlens diameters (hexagonal packed arrangement) for various spin speed experiments. As an example, in the grey zone corresponding to microlenses with diameters between 70 to 80 microns, NA between 0.07 to 0.14 have been realized by changing the spin speed and/or the dilution of the photoresist.

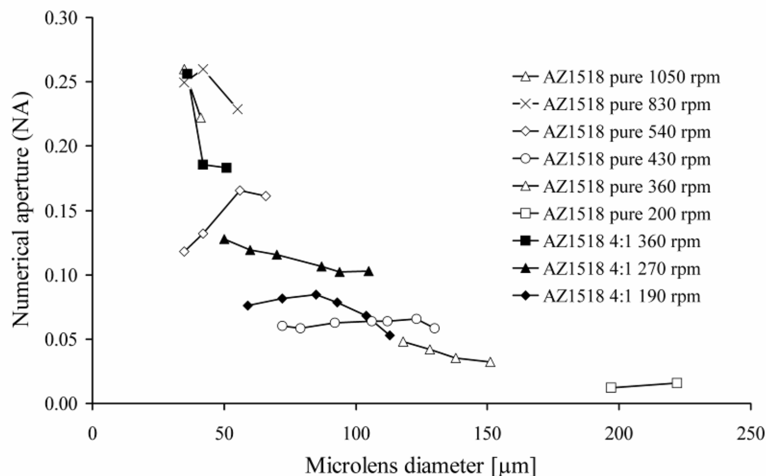

Fig. 6. Numerical aperture (NA) function of the microlens diameters (square packed arrangement) for various spin speed experiments.

As an example square packed concave microlens arrays of pitch between 70 to 80 µm with a gap of 10 µm having NA from 0.07 to 0.14 have been realized (grey zone in Fig. 5). The differences observed in the results presented in Figs. 4-6 between square and hexagonal packed microlens arrays could come from the boundary conditions imposed by the geometry

#102197 - $15.00 USD Received 29 Sep 2008; revised 31 Oct 2008; accepted 2 Nov 2008; published 11 Nov 2008
(C) 2008 OSA

of the melted holes. The influence on the resulting meniscus shape of these boundary conditions is shown in Fig. 7.

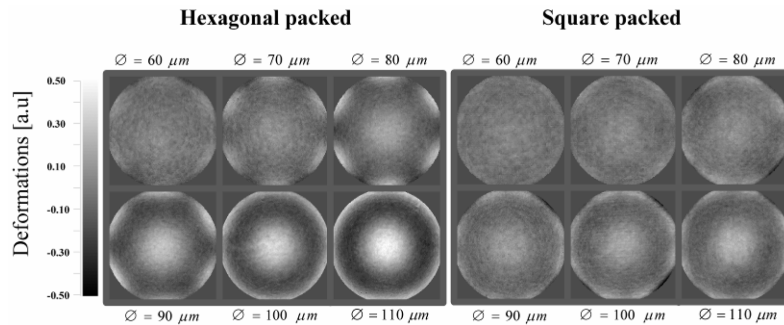

Fig. 7. 2D profile deformations from a sphere for increasing microlens diameters from 60 to 110 µm. The arrangement of the array is clearly seen in the deformations which occur at the four cardinals points for square packed array and at both sides of the three axis of symmetry for hexagonal packed microlens array. The first photoresist layer is 17 µm of AZ4562 and the second layer of diluted (4:1) AZ1518 was spin coated at 360 rpm.

The figure shows RMS deformations from a sphere occurring for increasing diameters after deposition of the second layer (AZ1518 4:1 270 rounds per minute (rpm)). For diameters lower than 80 µm no significant deformations are visible (Strehl ratio ~ 96 %). For diameters between 80 µm and 100 µm deformations are clearly visible as well as their different locations for hexagonal and square packed arrays. In this experiment square packed microlens arrays are less sensitive to the boundary conditions. For diameters Ø = 100 µm the holes are not enough filled and after drying both (square and hexagonal packed) microlenses exhibit similar deformations. Figure 8 shows the profile formation of the concave shape in measurements performed on a constant microlens diameter Ø = 50 µm and for different spin speed experiments.

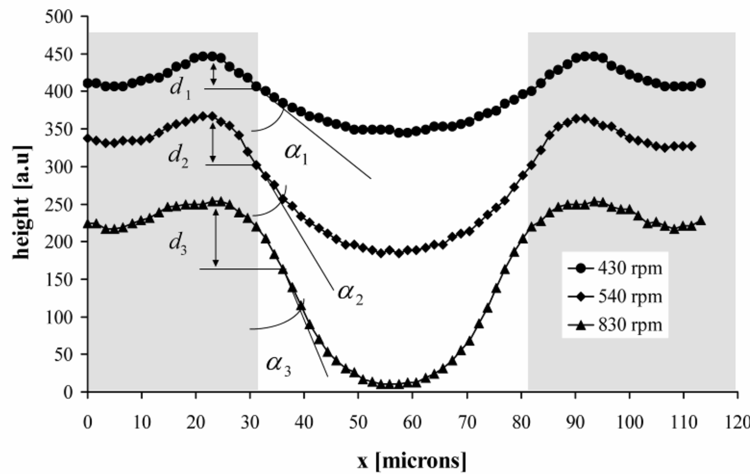

Fig. 8. Profile measurements of concave microlenses with Ø =50 µm (white area) obtained at 3 spin speeds of pure AZ1518. The vertical positions are set arbitrary. The anchoring point (i.e., the inflection point of the profile of the microlens) of the meniscus will depend on the filling of the holes. As it can be seen the distances (d_1, d_2 , d_3) between the top part of the profile and the starting slope (α_1, α_2, α_3) of the meniscus decrease. At 830 rpm the meniscus starts within the hole and deformations appear at the edges as shown previously in Fig. 7.

#102197 - $15.00 USD Received 29 Sep 2008; revised 31 Oct 2008; accepted 2 Nov 2008; published 11 Nov 2008
(C) 2008 OSA

Because of the non-vertical walls surrounding the meniscus, the radius of curvature (ROC) of the realized microlenses changes in correlation with the fill rate of the holes. An important question is the homogeneity of the obtain results. For spin speeds higher than 2000 rpm some shadow effects of the structures, mainly coming from additional reference structures between the microlens arrays, are observable. For lower spin speeds the results are quite homogenous even if the tested wafers contained various structures in height and size. Figure 9 shows a homogenous array of several microlenses.

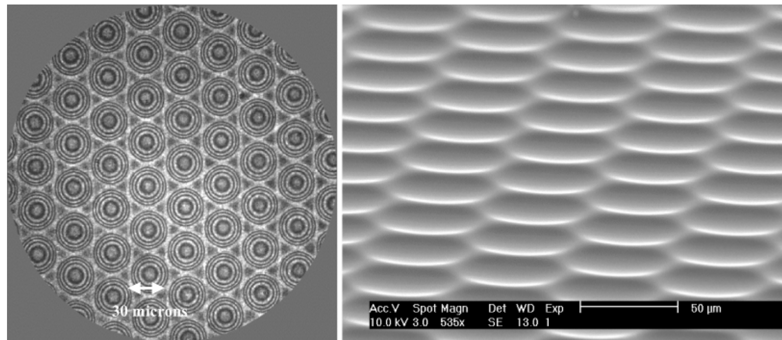

Fig. 9. Large scale interference picture and SEM picture of respectively 40 µm pitch and 60 µm pitch concave microlens array showing the homogeneity of the realized samples.

The typical defects encountered during the fabrication process are illustrated in Fig. 10. It consists in trapped air bubbles, dust particles, cracks in the second layer as well as local adhesion problems of the first layer. At very low spin speeds it is necessary to remove the photoresist at the edge of the wafer during the spinning to ensure a homogenous distribution of the second layer. The reproducibility of the experiment is closely linked to the quality of the photolithography of the first layer. Once the thickness, the parameters of the exposure and the development of the photoresist are kept constant, variations of less than 6% were observed on the focal length of the diffraction limited microlenses.

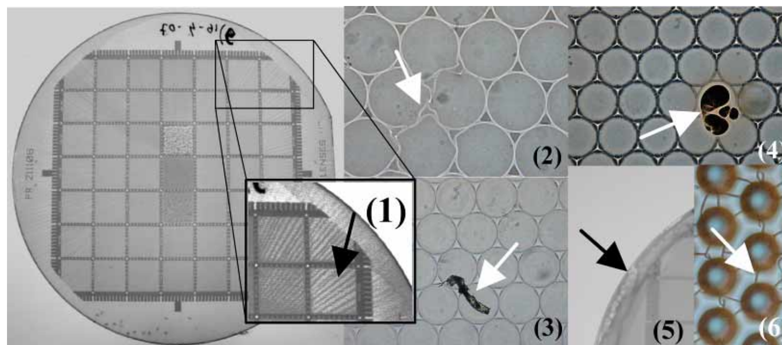

Fig. 10. Pictures of typical defects encountered during the fabrication process. (1) Shadow effect of the structures during spinning of the second layer of photoresist for spin speed higher than 2000 rpm. (2) Local deformation due to local weak adhesion of the first layer. (3) Dust particles. (4) Trapped bubbles. (5) Edge beads formation of photoresist at very low spin speed of the second layer (< 400 rpm). (6) Cracks in the second spun layer.

The temperature, as well as the dilution rate of the photoresist used to fill the holes, are important parameters which have to be well controlled. Because of the required melting step in the fabrication process, the surfaces between microlenses are not flat.

#102197 - $15.00 USD Received 29 Sep 2008; revised 31 Oct 2008; accepted 2 Nov 2008; published 11 Nov 2008
(C) 2008 OSA

4. Concave microlens diffusers

The diverging lens shapes offer the advantage of avoiding the formation of local "hot spots" (i.e. strong local intensity distribution) when illuminated. We used this property to realize diffusers in the perspective of beam shaping application for high power lasers applications. Moreover, in contrary to the case of microlens arrays, the smooth profiles of the areas between microlenses are interesting, because they reduce zero order transmission of the light. The hole pattern is shown in Fig. 11. In the left part of the figure, the range of diameters varies from 100 µm to 300 µm (RCL 4). In the center part, the range of diameters varies from 70 µm to 160 µm (RCL 5) and from 160 µm to 500 µm (RCL 6) in the right part.

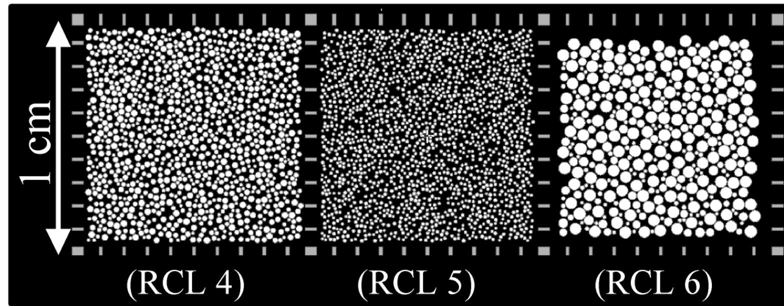

Fig. 11. Illustration of the three patterns of randomly distributed holes. The diameters of the holes were contained in ranges from 100 to 300 µm (RCL 4), 70 to 160 µm (RCL 5) and from 160 to 500 µm (RCL 6).

Using a Mach-Zehnder interferometer, the profiles of three different diffusers were measured and shown in Fig. 12.

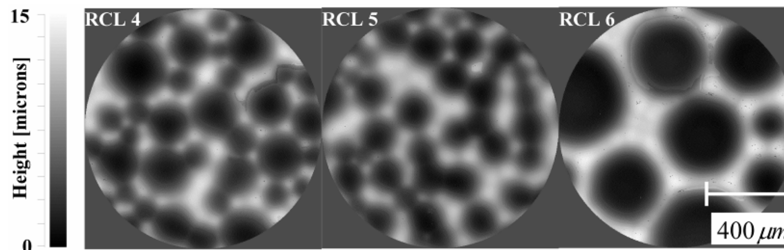

Fig. 12. 2D profiles of three realized diffusers. Because of the reflow occurring during the melting step of the first layer the zones between concave microlenses are no more flat and show a strongly reduced zero order transmission. The first layer is set to 17 microns and the second layer of pure AZ1518 has been spin coated at 200 rpm.

The typical depth of the resulting structures was around 15 µm. To avoid a strong zero order transmission of the diffusers, the main part of the holes must be filled to form concave shapes. Because of the large hole diameters (designed to ensure low diffusing angles), only very low spin speed fulfilled this condition. The diffusing properties of the random concave microlens diffusers have been analyzed using a goniometric setup. The results are shown in Fig. 13. While most of the measured diffusers only scatter around 10% of the light intensity and have a strong zero order transmission, two diffusers (AZ1518 pure 200 rpm RCL 4 and RCL5) show a smooth distribution of the transmitted light with a cut-off angle around 4°.

#102197 - $15.00 USD Received 29 Sep 2008; revised 31 Oct 2008; accepted 2 Nov 2008; published 11 Nov 2008
(C) 2008 OSA

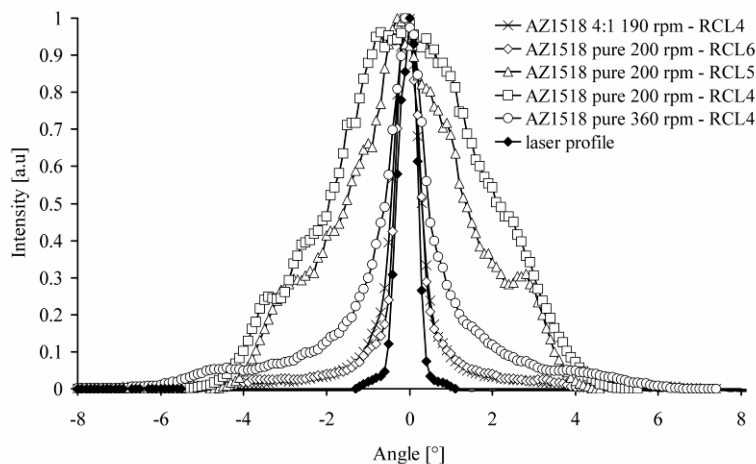

Fig. 13. Measured angular distribution curves of concave microlens diffusers. AZ1518 pure 200 rpm RCL 4 and RCL5 show very nice smooth dispersion while no significant zero order transmission is observable.

5. Conclusion

A two step method allowing the fabrication of diffraction limited concave microlens arrays has been demonstrated. Concave microlens arrays from 40 to 240 µm pitch with fill factor up to 80% were realized. Moreover by adjusting the process parameters of the photoresist a control of the numerical aperture NA is possible (from 0.07 to 0.14 for a microlens diameter of 70 µm). These lenses can be replicated using soft embossing techniques or could be transferred into fused silica wafers by dry etching. The fabrication process of concave microlenses has been successfully applied to the realization of diffusers. The diffusers generate a light distribution with 4° cut off angle and show almost no zero order transmission.

#102197 - $15.00 USD Received 29 Sep 2008; revised 31 Oct 2008; accepted 2 Nov 2008; published 11 Nov 2008
(C) 2008 OSA